Optical Tracking of Artificial Earth Satellites with COTS Sensors

Tanner S. Campbell
Department of Aerospace and Mechanical Engineering, University of Arizona, 1130 N Mountain Ave, Tucson, AZ 85721

Prof. Vishnu Reddy
Lunar and Planetary Laboratory, University of Arizona, 1629 E University Blvd, Tucson, AZ 85721

Prof. Jeffrey Larsen
Department of Physics, United States Naval Academy, 572C Holloway Road, Annapolis, MD 21402

Dr. Richard Linares
Department of Aeronautics and Astronautics, Massachusetts Institute of Technology, 77 Massachusetts Ave, Cambridge, MA 02139

Prof. Roberto Furfaro
Department of Systems and Industrial Engineering, University of Arizona, 1127 E James E. Rogers Way, Tucson, AZ 85721

ABSTRACT

Tracking of artificial Earth satellites is typically performed with ground based radar but newer commercial off-the-shelf (COTS) optical sensors are a valuable complementary technique. Optical sensors are sensitive to the weather but newer systems are inexpensive, can be operated autonomously and while they not only can perform initial orbit determination (IOD) they also add the benefit of providing rotational information via photometry. This makes the ability to track and observe Earth satellites much more accessible to the research and academic community. In this paper we present our automatic astrometry pipeline for reducing COTS optical sensor data from three main orbital regimes (low, medium, and geosynchronous). We present the successful pipeline with preliminary observations of multiple artificial Earth satellites, including the now defunct Chinese space station, Tiangong 1, shortly before atmospheric reentry. Development and calibration of the pipeline continues, with the most important focus being characterization of the sources of error to improve our astrometric and photometric accuracy. Observations of the geostationary telecommunication satellites GALAXY 15 and ANIK F1R are compared to predicted locations using published ephemeris showing a good characterization of the errors present in our system. Our astrometric solutions for Tiangong 1 are compared to predicted locations using less accurate, two-line element (TLE) data since no published ephemerides are available. This type of analysis gives a qualitative characterization of systematic errors in our process. Finally, we compare our astrometric solutions to catalog star positions to characterize the limiting positional noise in our current system so that we have a baseline metric to which we can compare future improvements.

1. INTRODUCTION

As more nations become active in space the burden on our current tracking systems will worsen. There is a real need for precise, inexpensive, autonomous tracking systems with the potential for global coverage. Radar provides useful information for tracking Earth orbiting satellites, but there are some shortcomings that can be improved upon with optical observations. The largest of these is the cost associated with operating radar tracking for SSA. Optical systems can be operated autonomously and are far less expensive to operate. While optical observations lack range information, there is no shortage of methods proposed for angles-only orbit determination meaning that they can be a useful supplement to radar tracking and alleviate some of the burden [1], [2], [3], [4], [5]. Using commercial off

the shelf (COTS) components, it is now possible to build inexpensive optical telescopes that can provide precise object tracking.

In this paper, we demonstrate the usefulness of COTS optical systems for tracking artificial Earth orbiting satellites in the three main orbital regimes (LEO, MEO, and GEO). We present the relative hardware details about sensors and optics for our three telescopes in Section 2. Section 3 discusses some data collection philosophy and considerations to derive the most useful products from your observations. Following this in Section 4 is a brief summary of methods used in our astrometric reduction process and automatic object detection. Section 5 is an initial analysis of the systematic errors present in our current system using observations of several GEO satellites as well as the defunct Chinese space station, Tiangong 1.

2. HARDWARE

The data used for this research was collected with three optical sensor systems. Their basic sensor characteristics can be found in Table 1. The two Finger Lakes Instrumentation (FLI) cameras each use a Light Pollution Reduction (LPR) filter, necessary due to their location within the city limits of Tucson, AZ. The PL16803 has a front illuminated 4K monochrome CCD sensor with 9 μm pixels that has a peak Quantum Efficiency (QE) of 60% at 550 nm [6]. The PL4710 is a back illuminated deep depletion 1K monochrome CCD sensor with larger 13 μm pixels that has a QE of over 90% at 800 nm [7]. Finally, the QHY174M has a 2K monochrome CMOS sensor with 5 μm pixels that has a peak QE of 70% at 530 nm [8]. Image time comes from a Sidereal Technology (SITECH) GPS time server with 0.5 millisecond accuracy, however currently this is truncated to the nearest second by the camera control software [9].

Table 1. Telescope and camera parameters that were used to collect data for algorithm and method testing.

Name	Aperture (m)	Focal Length (m)	Camera	FOV (deg)	Pixel Scale (as/px)
RAPTORS	0.610	2.831	FLI ProLine 16803	0.73x0.73	0.64
Leo-20	0.521	1.523	FLI ProLine 4710	0.5x0.5	1.76
Wide FOV	0.027	0.050	QHY174M-GPS	13x8.2	24.17

3. DATA COLLECTION

While the method used to track and collect data on artificial Earth satellites is flexible, it also can be the largest source of systematic error on the derived positions. In addition to the obvious physical factors of the camera and surrounding environment that have an effect on the quality of observations, the actual *way* the data was collected is important as well. For the purposes of optical observations of artificial satellites in Earth orbit, there are three main methods to consider: object rate tracking, sidereal tracking, and staring.

Staring is mainly useful for fast moving object detection and is where a wide field of view (FOV) telescope "stares" at the sky with a fixed orientation relative to an Earth fixed frame (stationary telescope pointed low on the horizon). Exposure time, which will be discussed later, is a key factor here. Ideally, using a high frame rate and short exposures will allow any fast moving object *and* the background stars to be approximately point sources in the images, yielding a good astrometric solution. Without a high frame or short exposures, objects will be streaks on the image. This is not all bad since it allows for rapid identification and potential targeted follow-up observations, but cannot be used for precise astrometry. Having precise time information is crucial for this type of observation. Our wide FOV setup fulfills all of these requirements with a short focal length capable of capturing fast moving LEO satellites; however due to the large pixel scale it is better suited to initial object detection than precision astrometry.

Sidereal tracking is used to keep the star background stationary in the images. The telescope moves at a rate equal and opposite to the Earth's rotation relative to the stars which means that the stars in each image will appear as point sources (gives a good plate solution) and any Earth orbiting satellites will appear as streaks. The length of the streak is determined by exposure time, object orbit, and pixel scale. This is a another convenient way to take

observations of satellites if the telescope mount cannot move fast enough to rate track the object, and may actually be preferred over object rate tracking due to the accuracy of the plate solution. When observing GEO satellites, it is possible to use either rate or sidereal tracking and achieve similar solution accuracy if the exposure time is kept below 0.5 seconds. Since the relative speed between sidereal tracking and geosynchronous tracking is so low, a short exposure can give point source detections for stars and GEO satellites, the best case to yield a good astrometric solution.

Lastly, there is rate tracking. This method requires a priori knowledge of the object to be observed (where the previous two methods can be used opportunistically). To rate track, an estimate of the object's transverse rate across the sky is needed, as well as a location and time; all of which may come from ephemeris, TLEs, staring prediction, or other methods. The accuracy of the plate solution for this observation method depends largely on exposure time, accuracy of a priori information, and precision of telescope mount. Since tracking is at an Earth orbiting object's transverse rate, the stars in the background will typically be streaked (length of streak depends on exposure time and transverse rate of the satellite). This makes the plate solution more difficult and will typically be slightly less accurate than that of sidereal tracking unless the exposure time is short enough to keep a round point spread function (PSF) for the background stars. If the a priori information on the object is not very precise or is inaccurate, it is possible to miss the object entirely, have streaks that start or stop out of image frame (unreliable centroid/rate estimation), or have "wobble" in the object footprint on the image. Moreover, any of these issues can be adversely affected by the precision of the observing equipment. Streaking and object wobble can be minimized by short exposure times and/or observing slower moving objects (such as geostationary satellites). The only way to combat poor a priori information is with a high observing cadence (many frames per second) and a large field of view. Often there is a compromise that must be reached in this regard and the fact that some objects may be missed given poor a priori information must be accepted.

Regardless of the choice of method, exposure time plays a key role in the quality of the final astrometric and photometric solution. The exposure time depends critically on several variables: detector well depth, object transverse rate, mount movement speed, and accuracy object of a priori information (if applicable, i.e TLEs). An ideal case from an astrometric point of view would be to have an exposure time of a sidereal tracked image such that the object crosses exactly one pixel. This yields the best plate solution (point source stars), as well as the most precise and simplest centroid calculation of the object. In this theoretical image, there are no streaks to deal with and all positions can be precisely determined at exposure mid-point. Some of the factors which influence the exposure time, t_E, are shown in Eq. (1):

$$t_E = \frac{p_x h}{f' v_s} \tag{1}$$

Where p_x is the size of a detector pixel, h is the altitude of the object's orbit above the observation station, f' is the focal length of the telescope, and v_s is the object's orbital speed. Since Eq. (1) does not consider the number of photons absorbed by the detector in that time, it is quite possible that the time t_E is too short for a "sufficient" detection.

A more detailed calculation can be done estimating the amount of returned photons during this exposure time, and comparing this to a desired signal to noise ratio (SNR) can yield a minimum exposure time for (good) detection of the object in the image. Since this is, almost as a rule, longer than t_E, the object will have crossed more than one pixel in that time (streak) and there is now ambiguity about the precise object location in the image. A common approximation is that the object position is in the midpoint of the streak at the midpoint of the exposure, which alleviates this ambiguity. However, this makes some assumptions about the relative motion between the spacecraft and telescope, and does not allow for multiple detections of the same object in a single streak. In reality, artificial Earth satellites are often too small/dim to be detected in t_E and there are other factors to be taken into account to decide on exposure time.

On the opposite end of things, too long of an exposure can not only cause streaks in the image, but can saturate the detector well which makes centroid estimation and photometry unreliable. There are many things that affect the exposure time decision, and it is very dependent on the observation station setup so experimentation is the best method for selecting effective times.

4. DATA REDUCTION

Our astrometric reduction process is designed for a UNIX-based operating system so that it can be easily scaled for distributed use on High Performance Computing (HPC) systems for rapid analysis of large datasets. To ensure support of a wide array of observations from diverse locations, our reduction pipeline is capable of matching stars with 24 different star catalogs including the recently released massive GAIA DR 2 catalog [10], [11]. Star and object centroids are computed using an iterated isophotal first-order moment with second-order correction given in Eq. (2). The iteration is initialized with a simple isophotal first-order moment, ${}^{(0)}\bar{x}_i$, and follows the scheme:

$$ {}^{(k+1)}\bar{x}_i = {}^{(k)}\bar{x}_i + 2\frac{\sum_j {}^{(k,j)}w^{(j)}I({}^{(j)}x_i - {}^{(k)}\bar{x}_i)}{\sum_j {}^{(k,j)}w^{(j)}I} \tag{2} $$

Where $i \in \{1,2\}$ denotes the axis of the centroid coordinate (i.e. 'x' or 'y'), k is the iteration index, and j is the summation index over all pixels that belong to a given image object. The ${}^{(j)}I$ are the pixel values and the ${}^{(k,j)}w$ are given by:

$$ {}^{(k,j)}w = \exp(-\frac{{}^{(k,j)}r^2}{2\sigma^2}) \tag{3} $$

In Eq. (3), ${}^{(k,j)}r$ is just the Euclidean distance between each pixel in the object and the previous centroid location, and σ is the diameter that contains half of the object flux in the image divided by $\sqrt{8ln2}$. The centroid position is iterated until the change between iterations is less than two ten-thousandths of a pixel (approximately 3 iterations).

This method is chosen because it is more accurate than a simple isophotal centroid, and faster than Point Spread Function (PSF) fitting with very similar accuracy (close to the limit of image noise). Once the pixel locations of the centroid of all light sources in the image are extracted, their relative spacing is cross-correlated with that of stars from the desired catalog. This yields the plate solution for a given image describing the mapping between our camera frame on the sky and a topocentric celestial angular coordinate frame (right ascension and declination). With the plate solution completed, the image goes through a more detailed conditioning and centroid extraction process to provide not only the pixel locations, but celestial coordinates of light sources in the image. A precession correction using the FK5 system is applied to these coordinates so that they are expressed in the J2000 frame.

With a direct mapping between camera frame and J2000 celestial coordinates, along with very precise centroid information, the actual "measurement" of the desired object(s) in the image is simply a matter of identifying their location in the image frame. This can be done automatically or by hand depending on the researcher's desires, and the exact method depends directly on the data collection process used (as described in the previous section) and type of object observed (i.e. orbital regime).

5. DATA ANALYSIS

To characterize the error level present in our current system we can use several different methods. To understand the overall noise in our observations, we can compare the published catalog position of stars in our images, with our astrometric solution for those stars. The average of the star position residuals for each image in a sequence of observations can give a good characterization of the noise level in the solution. Fig. 1 shows a plot of these average residuals for two different data sets.

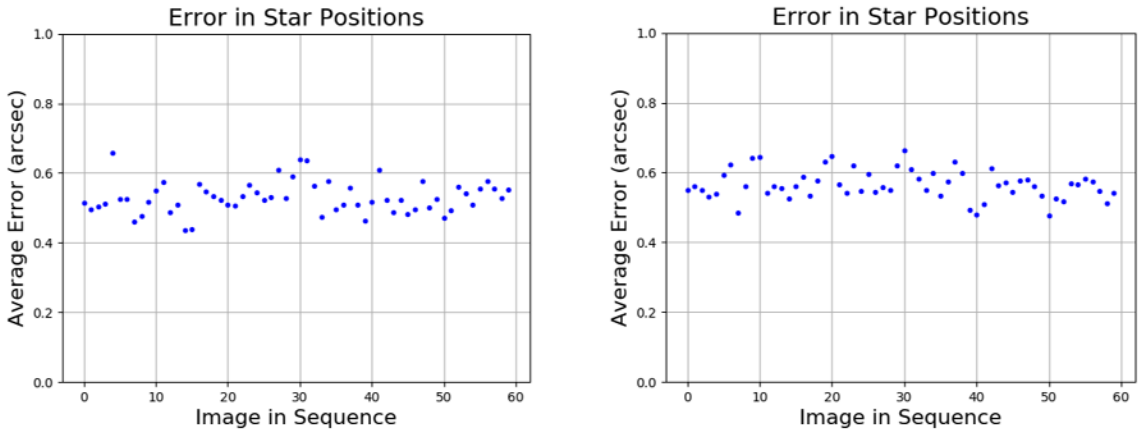

(a) (b)

Fig. 1. The average residual for star positions in 120 images collected on June 6, 2018 of GALAXY 15 (Fig. 1a) and ANIK F1R (Fig. 1b) taken with the Leo-20 telescope. Residuals are calculated from GAIA DR2 catalog positions and averaged over each image frame.

Using the two plots in Fig. 1 as a baseline metric, we calculate between 0.4 and 0.7 arc-seconds of noise in our astrometric solutions for these data sets. To see if there is any appreciable bias in our solutions, we can look at the individual star errors for a given image. Looking at a handful of the brightest stars in an image we can see in Fig. 2 that all the star position errors are approximately Gaussian about zero. Spot checking other images in our data sets gives similar results implying that there is not a significant bias in our astrometric reduction. However, from Fig. 2 it is clear that while the average star position residual is sub arc-second, some star position solutions are relatively poor. Using a deeper scan of the image for dimmer stars, it is expected that this spread would increase. We can attribute this spread in star position error largely to astronomical seeing, which is estimated to be about 2.5 arc-seconds for a common night with this telescope (Leo-20) due to its location within the city of Tucson, AZ.

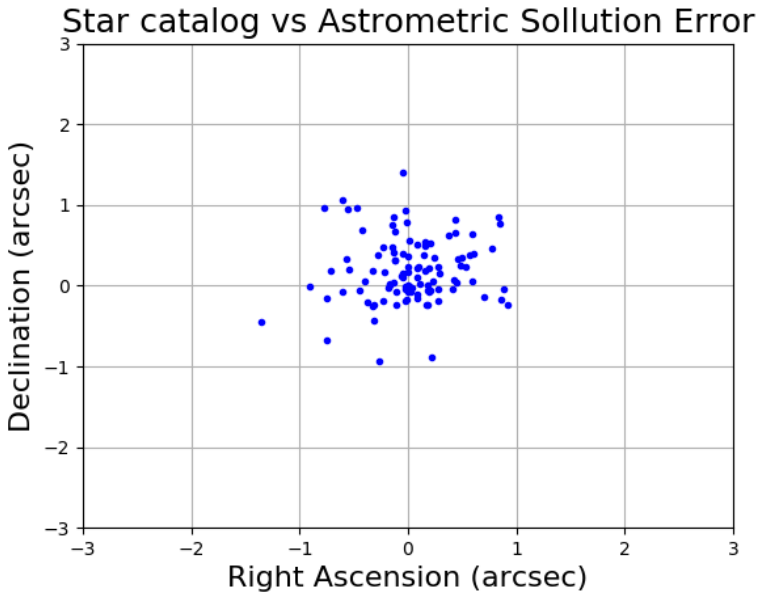

Fig. 2. The individual errors in the brightest star positions for a single image taken on June 6, 2018 of GALAXY 15 with the Leo-20 telescope.

With a baseline accuracy established for our plate solutions, we can turn our attention to the actual objects we observed. The difficulty with analyzing observational accuracy of Earth satellites is having "truth" positions to evaluate your observations against. Conveniently, GPS satellites publish very accurate ephemeris that can be used to compare results to, however to date we have not observed any GPS satellites. Our main focus has been on geosynchronous satellites. There are a handful of GEO satellites that also publish very accurate ephemeris publicly available through the FAA NSTB database, among which are GALAXY 15 and ANIK F1R. Fig. 3 is a comparison of the published ephemeris of GALAXY 15 with 60 observations from a single night.

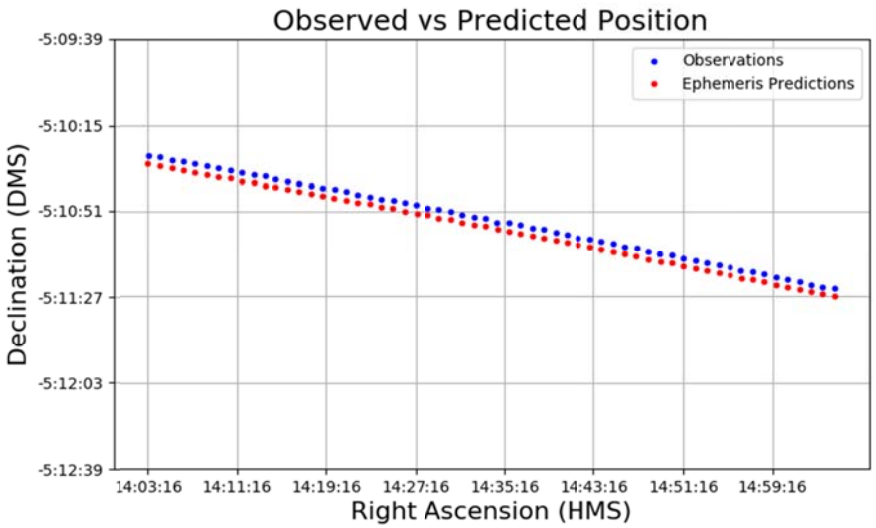

Fig. 3. Comparison between published ephemeris for GEO satellite GALAXY 15 and our astrometric solutions from data taken on June 6, 2018 with the Leo-20 telescope.

Looking more closely at the residuals between the two positions (Fig. 4), we can see some systematic errors in our measurement of this object. Across the whole data set there is an almost constant positive bias in declination on the order of 3 arc-seconds, and a spread in right ascension errors from -10 to 7.5 arc-seconds. Analysis of data collected of GALAXY 15 on the following two nights shows an almost identical story.

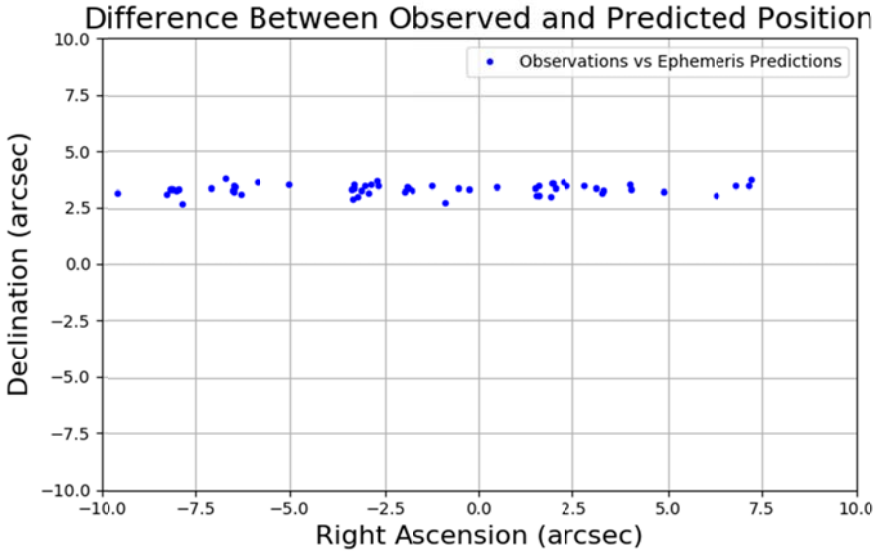

Fig. 4. Position error residuals for our observations of GEO satellite GALAXY 15 from June 6, 2018 with the Leo-20 telescope.

Since we did not see this type systematic error in star positions, we can make some assumptions about the source of this error. For instance, approximating a GEO satellite's transverse rate at 15 arc-seconds per second, we can equate the spread in right ascension to approximately a ± 0.5 second timing error. Further analysis of our timing setup revealed that even though we were using a very accurate GPS time server, the image time was only being stored in the image header to the nearest second, yielding a ± 0.5 second uncertainty. We are currently in the process of updating the camera control software to store time with millisecond precision.

The bias in declination is harder to explain, but we suspect that it could potentially come from both poor precision and accuracy in observation site location. At present we have observation site location precise to 0.00014 degrees in both latitude and longitude (approximately 30 m in each direction), and to 1 m in altitude. However, we do not have a good bound on how accurate these measurements are, and a very small error in latitude or altitude would be enough to explain all of the declination bias (most likely it is a combination of the two). In order to accurately compare the satellite ephemeris to our observations, we must also accurately compute our site position in vector form, to do this we use an average Earth radius of 6378.137 km and flattening of 0.081819221456 as suggested in [5], but it may be the case that either of these is not appropriate for our location.

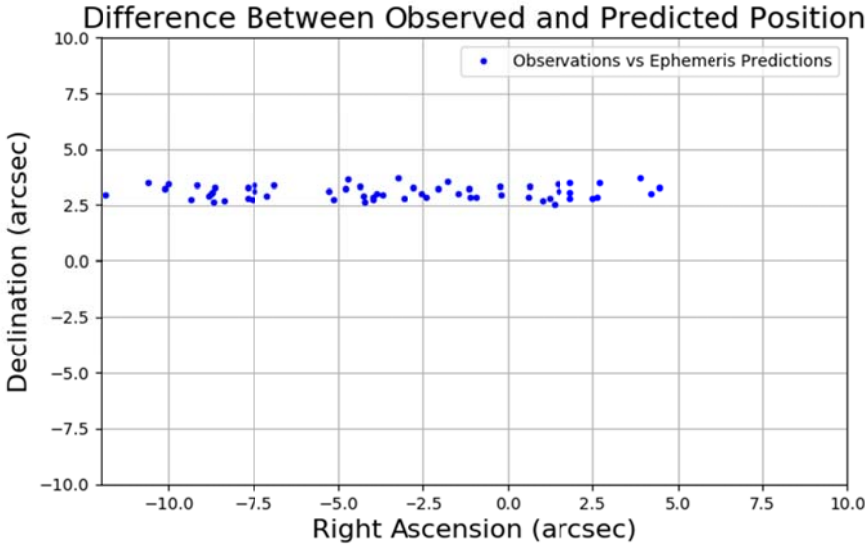

Fig. 5. This is analogous to Fig. 4, but the observations are of ANIK F1R on June 6, 2018.

Performing a similar analysis with ANIK F1R shows that these errors we see with GALAXY 15 are indeed systematic. We likewise observed ANIK F1R for three consecutive nights, and as with GALAXY 15, all three nights show approximately the same errors. While errors are not ideal, these types of systematic errors can be eliminated almost in their entirety with future datasets, meaning that we will expect to see errors of the same order as our star position uncertainty (approximately 0.5 arc-seconds). Once the systematic errors have been removed, we can focus on improving our reduction process to hopefully reduce our star position uncertainty as well.

Since most GEO satellites do not publish their ephemeris for the public, the orbit information that can be used to compare observations to is from TLEs. These are publicly available for unclassified satellites thanks to Space-Track and can be used for coarse, short-term, satellite location prediction. Due to the precision limitations of the TLE format, for the purposes of error analysis all we can do is qualitatively check or results to make sure they are reasonable. Fig. 6 is a comparison of observations of the Chinese space station, Tiangong 1, a few months before it reentered our atmosphere to the published TLE on that day.

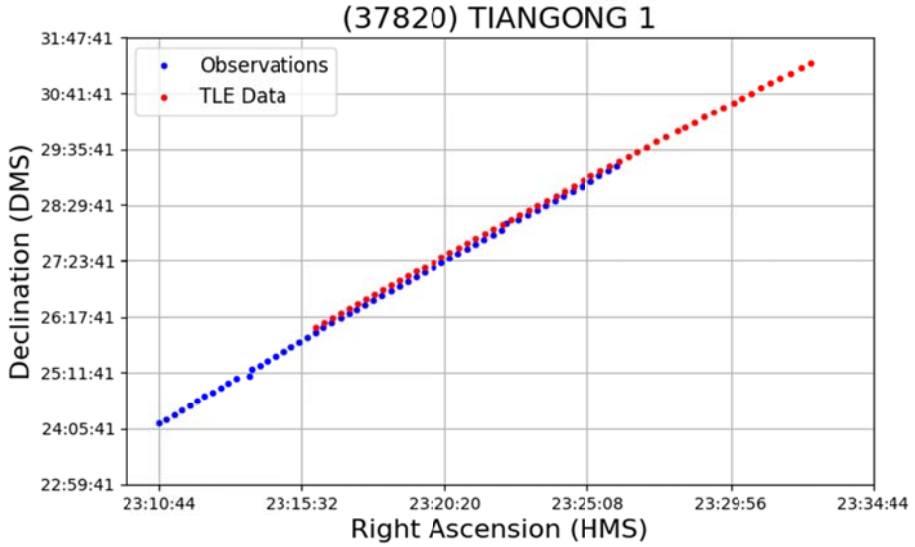

Fig. 6. Comparison of predicted locations of the Chinese Space Station, Tiangong 1, using the Space-Track published TLE on January 12, 2018 and our observations with the Wide FOV telescope. NOTE: There was a problem with our time server during the collection of this data.

It is obvious from Fig. 6 that there is a significant timing error with this data, and yet unlike the previous data we discussed, this is not due to poor time precision in our image headers. In this case, time is not truncated to whole seconds, but is full accuracy. This is why the timing error can be seen as a bias rather than a distributed uncertainty. The timing error in this case comes from a failure of the time server to connect and accurately set the image times resulting in a roughly constant offset between our system time and GPS time. By aligning the beginning points of each of the data sets in Fig. 6, we can see that there is also a drift in the position error (Fig. 7). This drift could be from our system, the accuracy of the TLE, or any combination of the two.

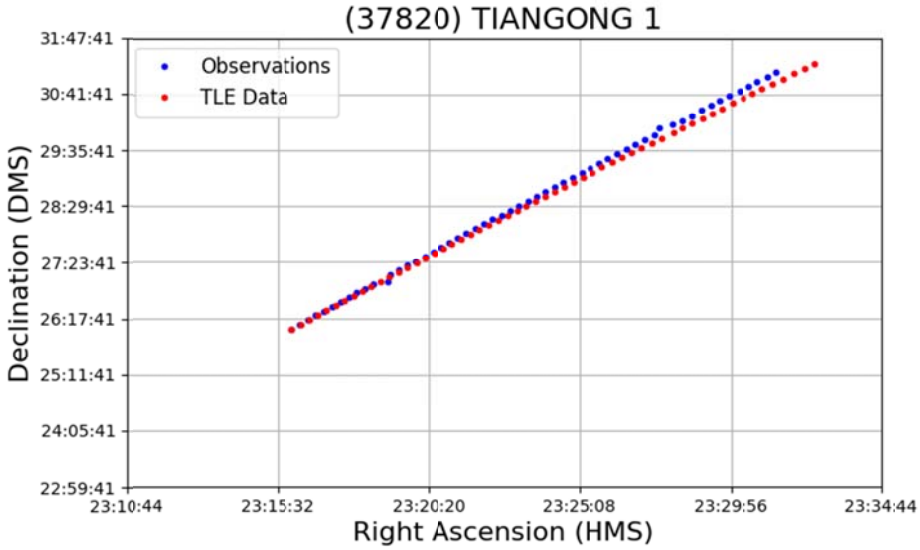

Fig. 7. Correcting for the initial timing offset found in Fig. 6 shows that in addition to this bias, there is a timing drift that could be from our system, the accuracy of the TLE information, or both.

6. CONCLUSIONS AND FUTURE WORK

We have demonstrated that high quality astrometric measurements can be obtained using small telescopes operated by students in an academic environment. As noted earlier, our primary focus has been to track down the source of systematic errors to bring our astrometric solutions of satellite positions to the same level of accuracy as our star positions (0.5 arc-seconds). The next step is to optimize the automated reduction process. Right now the automated reduction works well for targeted observations, i.e. object(s) in the image is (are) known at the time of observation. It is capable of detecting and providing measured observations for "opportunistic" objects that were not targeted, but these objects are not currently being identified. This type of identification is something that we are prototyping and will hopefully include in the coming months.

7. ACKNOWLEDGMENTS

This work is supported by the cooperative agreement between the United States Air Force Research Lab (AFRL) and the University of Arizona (PI: Prof. Roberto Furfaro) and the state of Arizona Technology Research Initiative Fund (TRIF) grant (PI: Prof. Vishnu Reddy).

This work has made use of data from the European Space Agency (ESA) mission Gaia (https://www.cosmos.esa.int/gaia), processed by the Gaia Data Processing and Analysis Consortium (DPAC, https://www.cosmos.esa.int/web/gaia/dpac/consortium). Funding for the DPAC has been provided by national institutions, in particular the institutions participating in the Gaia Multilateral Agreement.

8. REFERENCES

1. K. J. DeMars and M. K. Jah, "Probabilistic initial orbit determination using Gaussian mixture models," *Journal of Guidance, Control, and Dynamics*, vol. 36, no. 5, pp. 1324-1335, 2013.

2. K. J. DeMars, M. K. Jah, and P. W. Schumacher, "Initial orbit determination using short-arc angle and angle rate data," *IEEE Transactions on Aerospace and Electrical Systems*, vol. 48, no. 3, pp. 2628-2637, 2012.

3. A. Milani, G. Gronchi, M. Vitturi, and Z. Knezĕvić, "Orbit determination with very short arcs. I admissible regions," *Celestial Mechanics and Dynamical Astronomy*, 90:57-85, 2004.

4. G. Tommei, A. Milani, and A. Rossi, "Orbit determination of space debris: admissible regions," *Celestial Mechanics and Dynamical Astronomy*, 97:289-304, 2007.

5. D. Vallado. *Fundamentals of Astrodynamics and Applications.* Microcosm Press, Hawthorne, CA, Fourth Edition, 2013.

6. Finger Lakes Instrumentation, "ProLine PL 16803," PL16803 datasheet, 2018.

7. Finger Lakes Instrumentation, "ProLine PL 4710 DD," PL4710DD datasheet, 2018.

8. QHYCCD, "QHY174M," QHY174M datasheet, 2018.

9. Sidereal Technology, "SiTech Time Server Manual," SiTech Time Server datasheet, 2018.

10. Gaia Collaboration et al. (2016): Description of the Gaia mission (spacecraft, instruments, survey and measurement principles, and operations).

11. Gaia Collaboration et al. (2018b): Summary of the contents and survey properties.